Bone Marrow Disease

20

Andrea Baur-Melnyk and Tobias Geith

Contents

Abstract

The bone marrow consists of active red marrow and inactive fatty marrow which is mainly situated in the extremities. Red marrow can be replaced by various conditions. Focal disease is easy to perceive; however, diffuse disease is often hard to detect. Gadolinium application can help for quantification of contrast enhancement. Based on the results of a control cohort, the enhancement of normal bone marrow showed great variations between 3% and 40%, mean 17% (in adults age >40 years). In patients with multiple myeloma, mean enhancement is significantly higher >40 Vol.%. Other diseases with stimulation of red marrow can simulate diffuse disease and also lead to an increase of contrast enhancement. Therefore the clinical background is of great importance when interpreting such exams. Quantitative whole-body MRI with ADC analysis might be a feasible diagnostic tool to assess the short-term treatment response in myeloma patients.

Measurements have also been performed for therapy control in patients with Gaucher's disease. Gaucher's disease is a disease of the reticuloendothelial system. The reduction of the fat cell content, which reflects the severity of the disease, can be measured quantitatively by the chemical shift method. A semiquantitative method is the BMB score, which is a combination of scoring systems of the peripheral skeleton and the axial bone marrow component in

A. Baur-Melnyk, M.D. (✉) • T. Geith, M.D. (✉)
Department of Radiology, University Hospital,
LMU Munich, Germany
e-mail: andrea.baur@med.uni-muenchen.de;
tobias.geith@med.uni-muenchen.de

patients with Gaucher's disease. It incorporates both the visual interpretation of the signal intensities and the geographic location of the disease on conventional MR images of the spine and femur.

Dynamic contrast-enhanced MRI (DCE-MRI) has the potential to noninvasively assess the microvascular structure of bone marrow. In patients with acute myeloid leukemia in complete remission, K_{ep} (efflux rate constant) measured with tracer kinetic modeling represents the contrast exchange between blood plasma and extravascular extracellular space. It is thought that bone marrow vessels and their endothelium should be normalized with reduced vessel wall permeability in complete remission, and therefore show low values of K_{ep}. Increased values for K_{ep} may indicate a high risk of relapse and were associated with shorter overall survival and relapse-free survival, as could be shown in an initial study.

A sometimes challenging question is the differentiation of acute osteoporotic and malignant vertebral fractures. In uncertain cases, quantitative diffusion-weighted imaging and chemical shift imaging can provide additional features to overcome the diagnostic limitations of morphologic signs in MRI.

20.1   Introduction

Magnetic resonance imaging (MRI) allows for a visualization of bone marrow components concerning fat and water-bound protons. In adults hematopoietically active "red marrow" is located in the central skeleton (spine, pelvis, proximal femur and humeri, thoracic cage, and the skull), while inactive fatty "yellow marrow" is located in the distal parts of the extremities and the epi- and apophysis. Normal red marrow has intermediate to high signal intensity on T1-w SE images, high signal intensity on T2-w TSE images, and low signal intensity on fat-suppressed images (e.g., STIR). This is consistent with the composition of red bone marrow by ~40% fat and ~40% water. Yellow marrow is predominantly composed by fat cells and collagen fibers and shows strongly high signal intensity on T1-w SE, T2-w TSE images and low signal intensity on fat-suppressed images.

Bone marrow can be replaced or infiltrated by various benign and malignant disease states (Plecha 2000). This can happen in a focal or a diffuse fashion. Focal disease is shown by focal low signal intensity on T1-w SE and usually high signal intensity on T2-w SE and fat-suppressed images. Neoplastic focal marrow infiltration can be due to metastases, myeloma, lymphoma, and primary malignant bone tumors. Benign focal marrow replacement can be due to hemangiomas (typical/atypical), focal fat islands or hematopoietic islands without fatty components within red marrow or in the periphery of the skeleton (Vande Berg et al. 2005). Focal disease is easy to perceive due to the high contrast to normal marrow. Measurements are usually not necessary.

It is much harder to detect diffuse marrow alterations. Diffuse neoplastic infiltration can be due to metastases, myeloma, lymphoma, leukemia, chronic myeloproliferative disease, and myelodysplastic syndrome. Benign diffuse signal alterations can be due to stimulated marrow: increased need for erythrocytes in, e.g., hemolytic anemia and chronic bleeding; increased need of leukocytes, e.g., in sepsis or chronic inflammations; or stimulated marrow due to drugs (e.g., erythropoietin, granulocytic growth factor, early status post chemotherapy). Since MRI cannot differentiate between water-bound protons in neoplastic cells or hematopoietic cells, MRI is unspecific and should only be interpreted in conjunction with exact clinical information (Nobauer and Uffmann 2005).

20.2 Myeloma

Since diffuse marrow infiltration is sometimes hard to detect, measurements concerning gadolinium enhancements have been performed. Multiple myeloma is a disease which shows diffuse infiltration in about 30–40% of cases. According to the amount of marrow replacement, the signal on T1-w SE images is reduced. In cases of high-grade diffuse involvement (>50 Vol.% in bone marrow biopsy), the signal intensity is nearly equal to the signal intensity of the intervertebral disc or muscle on T1-weighted SE images due to the increase of water and decrease of fatty components. In cases of intermediate grade of involvement in biopsy (20–50 Vol.%), the signal reduction is only moderate and often hard to diagnose.

Based on the results of a control cohort, the enhancement of normal bone marrow showed great variations between 3% and 40%, mean 17% (in adults age >40 years) (Baur et al. 1997) (Fig. 20.1). This is explained mainly by the variations of the fat cell content in normal marrow interindividually and the changes that occur during aging with an increase of fat. Patients with lower fat content, mainly younger patients, show a stronger gadolinium enhancement than individuals with a higher fat cell content. In another study gadolinium enhancement was correlated to

Fig. 20.1 Contrast enhancement in percentage. Interindividual variability of percentage of contrast enhancement in bone marrow in 87 healthy subjects

the grading of diffuse infiltration, neovascularization of bone marrow, and the fat/hematopoietic cell content in myeloma (Baur et al. 2004). In myeloma patients with an intermediate- or high-grade diffuse infiltration of the bone marrow, mean enhancement was significantly higher than in normal bone marrow ($p < 0.0001$). Also in patients with low-grade diffuse infiltration, gadolinium enhancement was significantly higher than in normal bone marrow ($p < 0.01$) but showed a strong overlap with normal bone marrow (Table 20.1). As a simple rule it can be stated that if the percentage increase of signal exceeds the limit of 40% in patient older than 40 years, this can be considered as pathologic. The reasons for increased enhancement in diffuse infiltration by myeloma were an increased microvessel density, increased cellularity, and a decreased fat cell content (Vacca et al. 1994; Aguayo et al. 2000; Rajkumar et al. 2000; Baur et al. 2004). The fluent transitions of the plasma cell content, the fat cell content and the microvessel density, as well as the fact that all three parameters contribute to contrast enhancement explain that no definite cutoff values can be found for contrast uptake in diffuse infiltrating multiple myeloma. In addition, the percentage signal increase after gadolinium administration does not reflect an absolute value of perfusion, since the contrast media diffuses quickly into the extracellular space.

To measure the gadolinium enhancement of the bone marrow, the MRI examination protocol should include sagittal T1-weighted SE sequences without fat saturation before and after intravenous gadopentetate dimeglumine (Gd-DTPA) administration (0.1 mmol/kg body weight, 0.2 ml/kg). The contrast medium should be given as a bolus injection followed by a saline flush. Scan parameters on the pre- and post-contrast T1-weighted SE sequences have to be identical; the values for receiver and transmitter adjustments have to be kept constant.
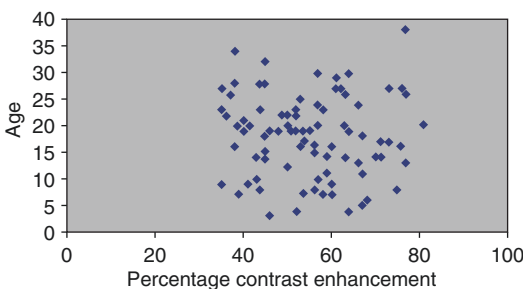
Table 20.1 Gadolinium enhancement in normal bone marrow and diffuse myeloma infiltration

Gadolinium enhancement	Normal marrow (%)	Low (%)	Intermediate (%)	High grade (%)
Mean enhancement	18	25	49	90
Standard deviation	8	10	19	30
Range	3–38	10–44	19–94	62–165

SI measurements should be made with circular region of interests placed in three vertebral bodies of the lumbar spine. The mean value should be calculated from the three measurements to compensate for SI differences within the bone marrow depending on changes in the ROI's position. Avoid placing the ROI's in midsagittal slices with basivertebral veins. The ROIs have to be placed in identical positions of the vertebral body on T1-weighted images before and after injection of contrast material (Fig. 20.2). The percentage SI increase is calculated as follows:

$$\text{Volume} = 4/3\pi \left(d/2 \right)^3$$

Previous studies in patients with lymphoproliferative disease demonstrated that *dynamic gadolinium-enhanced MRI* can distinguish malignant from normal bone marrow. In the study of Moulopoulos, focal infiltration of the bone marrow in various malignancies was examined (Moulopoulos et al. 2003). Mean wash-in and washout rates and the ratio between wash in and time to maximum slope were significantly higher in areas with focal infiltration than in controls. The study population of Rahmouni et al. comprised a mixture of 31 patients with multiple myeloma and Non-Hodgkin's and Hodgkin's lymphoma (Rahmouni et al. 2003). Maximum enhancement, slope, and washout on dynamic turbo fast low-angle shot sequences were significantly different for patients with bone marrow involvement versus controls. Time to maximum enhancement did not differ significantly. The enhancement time curve values increased with increasing bone marrow involvement grades.

With the introduction of anti-angiogenetic therapy contrast enhancement may play a role in monitoring disease status. First results of a clinical histological study in patients with multiple myeloma showed that the mean microvessel density was significantly lower in patients after chemotherapy in responders as opposed to non-responders. The progression-free survival was significantly longer than in patients without a decrease in microvessel density (Sezer et al. 2001).

Horger et al. examined the feasibility of whole-body diffusion-weighted MRI in the short-term evaluation of response to treatment in multiple myeloma patients using a single-shot EPI sequence in 12 patients using *b*-values of 50, 400, and 800 s/mm^2. Eleven patients were classified as responders and one as non-responder. DWI results accurately (100%) correlated with disease course according to standard clinical and laboratory criteria. At baseline, all lesions showed restricted diffusion; in responders ADC values had an increase of 63.9% (range −8.7–211.3%), while the non-responder had a decrease of 7.8% during therapy. In parallel, M-gradient measurement showed a mean decrease of 45.1% (range, 19.6–88.8%) in responders and an increase of 21.8% in the non-responder. Amplitude of response measured by the course of ADC values proved higher in the appendicular skeleton (99.8%) compared with the axial skeleton (54.3%) ($p = 0.037$). These initial results show that quantitative whole-body MRI with ADC analysis might be a feasible diagnostic tool to assess the short-term treatment response in myeloma patients (Horger et al. 2011).
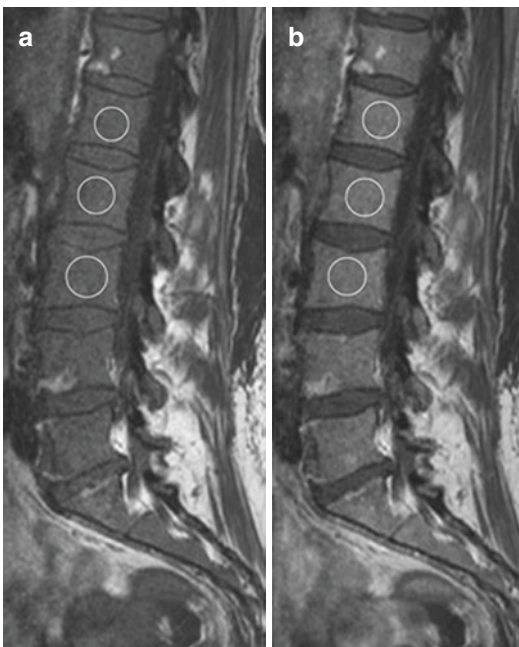

Fig. 20.2 T1-w SE image (TR/TE 572 ms/15 ms) pre- and post-contrast in a patient with diffuse infiltration by myeloma. The regions have to be placed in identical positions in lumbar vertebral bodies. Mean signal intensity increase can be calculated. An increase of more than 40% in adults (>40 years) is indicative of diffuse infiltration

20.3   Infectious Spondylitis

The typical pattern of infectious spondylitis is a hyperintense signal on T2-w images of the intervertebral disc, an early destruction of the adjacent vertebral endplates, and a vertebral bone marrow edema. Paravertebral and epidural extension, abscesses, and enhancement of the intervertebral disc, bone marrow, and surrounding granulation tissue may be associated. A study in patients with infectious spondylitis showed that systemic reactive marrow changes can simulate diffuse neoplastic infiltration similar to myeloma or chronic myeloproliferative diseases (Stabler et al. 2000). Due to a stimulation of leucopoiesis, the fat cell content in the bone marrow of the spine above and below the level of spondylitis is consecutively reduced. This leads to a decrease in signal on T1-w SE images, an increase on STIR images. Patients with infectious spondylitis showed a significantly higher mean enhancement of 28.2% (SD 12.2) when compared to a control group (mean enhancement 17.5%, SD 7.9, $p < 0.001$). This reactive bone marrow stimulation with increased gadolinium uptake occurred in 27% of patients with infectious spondylitis. Measurements were performed in the same way as described in patients with myeloma.

Another approach is the use of quantitative diffusion-weighted imaging. Pui et al. showed, that the mean ADC values of the bone marrow of 69 tuberculous ($1.15 \pm 0.39 \times 10^{-3}$ mm^2/s), 9 pyogenic ($1.30 \pm 0.45 \times 10^{-3}$ mm^2/s), and 50 malignant (1.02×10^{-3} mm^2/s) vertebral fractures were significantly higher, compared to normal vertebral marrow. Malignant bone marrow showed significantly lower ADC values than the ADCs of pyogenic infection or tuberculosis. No significant difference could be shown between adult ($1.15 \pm 0.42 \times 10^{-3}$ mm^2/s) and pediatric ($1.14 \pm 0.36 \times 10^{-3}$ mm^2/s) tuberculous lesions or between tuberculosis and pyogenic infection. For distinguishing infection from malignancy, they showed quite a low sensitivity, specificity, and accuracy of 60.26%, 66.00%, and 62.50%, using the cutoff ADC of $\geq 1.02 \times 10^{-3}$ mm^2/s. The overlap between ADC values for malignancy (probably due to different content of cells, protein, calcifications, or cytoplasm) and inflammation (probably due to different content of cells, mucoid protein, necrotic tissue, microorganisms, and pus) limited the usefulness of diffusion MRI in differential diagnosis, which was not able to obviate biopsy. But the sensitivity, specificity, and accuracy increased to 94.12%, 82.35%, and 90.20%, respectively, when there were associated soft tissue lesions with a cutoff ADC of $\geq 1.17 \times 10^{-3}$ mm^2/s (Pui et al. 2005).

20.4   Gaucher's Disease

Measurements have also been performed for therapy control in patients with Gaucher's disease. Gaucher's disease is a disease of the reticuloendothelial systems with a lack of the enzyme glucocerebrosidase. Glucocerebrosides accumulate in the reticuloendothelial system (bone marrow, liver, spleen, and lymph nodes). The infiltration of the bone marrow with Gaucher's cells leads to cell necrosis, fibrous proliferation, and resorption of bony trabeculae. The fat content of red marrow is reduced. In x-rays osteonecrosis and diffuse osteopenia can be found. In MRI the signal is diffusely reduced on T1-w SE images. In contrast to myeloma or leukemia, the signal is not increased on fat-suppressed images. The epi- and apophysis remain excluded of the process.

Quantitative Measurements Using the Chemical Shift Method

The reduction of the fat cell content, which reflects the severity of the disease, can be measured quantitatively by the chemical shift method. Dixon described a method to quantify the fat signal fraction by separating the individual signals from water and fat, F_f, hence Dixon quantitative chemical shift imaging (Dixon QCSI) (Dixon 1984). The QCSI technique has been explored in Gaucher's disease (Akkerman and Maas 1995; Hollak et al. 2001). The measured mean values in the lumbar spine (L3–L5) in healthy volunteers ranged from 0.27 to 0.55 (mean 0,37). In Gaucher's patients, the mean values ranged from 0.08 to 0.40 (mean 0.20). Bone complications, like bone crisis, fractures, and osteonecrosis, occur more often in patients with low fat fractions (<0.20), reflecting advanced disease (Maas et al. 2002).

A coronal measurement slice (if necessary slightly tilted to transversal) is set out on a sagittal localizer image, such that the posterior parts of the vertebrae of interest are optimally visualized (Fig. 20.3). The measurement is acquired using a surface coil. Two sets of acquisitions are performed, one of which the water signal (W) and

the fat signal (F) are "in-phase" ($I = W + F$). In the second acquisition, fat and water have opposed phases ($O = |W - F|$). In order to separate the water and fat signals, the phase difference between the two acquisitions helps to sort out regions with water-dominant signal and regions with fat-dominant signal. With the help of the sign image, water and fat images are obtained by simple algebraic manipulations. For the water image (W), we have $W = I + S \cdot O$ and for the fat image (F) we have $F = I - S \cdot O$. The fat fraction is described on a color-coded scale range from 0 (no fat) to 1 (all fat). The mean value of the vertebral bodies L3, L4, and L5 is the final fat fraction (Fig. 20.4).

Semiquantitative Measurements with the Bone Marrow Burden Score (BMB)

The BMB score is a combination of scoring systems of the peripheral skeleton and the axial bone marrow component (Maas et al. 2003). It incorporates both the visual interpretation of the signal
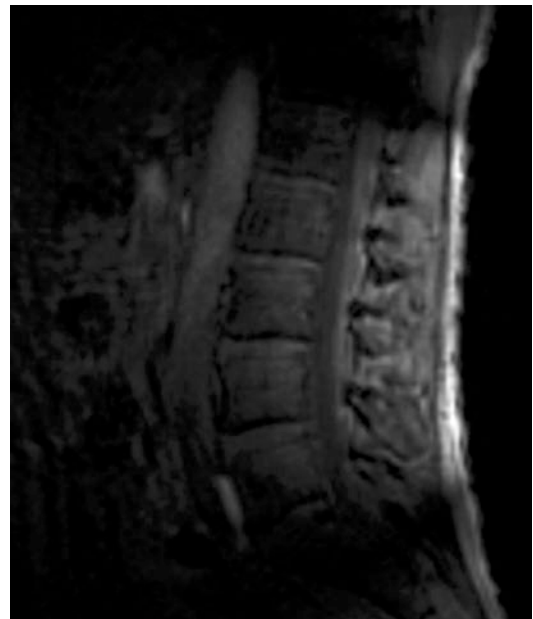

Fig. 20.3 Quantitative chemical shift imaging in a patient with Gaucher's disease. Placement of the localizer

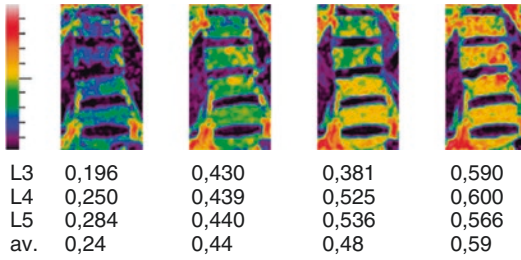|			
L3	0,196	0,430	0,381	0,590
L4	0,250	0,439	0,525	0,600
L5	0,284	0,440	0,536	0,566
av.	0,24	0,44	0,48	0,59

Fig. 20.4 Coronal color-coded display of fat fraction measurement in the lumbar spine, ranging from 0 (*purple*) to 1 (*red*). Patient with Gaucher's disease is measured pre- (*left image*) and subsequently three times (annually) during/after enzyme replacement therapy. Due to therapy success, the fat fraction is increased, which can be measured by chemical shift imaging. Low fat content is shown in blue to violet; high fat content is shown in *yellow* to *red*. With permission from Maas et al. (2003)

intensities and the geographic location of the disease on conventional MR images of the spine and femur. In the lumbar spine, the SI of the marrow on T1-weighted SE sequences is compared to signal intensity of a healthy intervertebral disc. The bone marrow SI on T2-weighted SE sequences was evaluated with the presacral fat as a normal isoin-tense reference. In addition the infiltration pattern (patchy versus diffuse) of the disease within the vertebral bodies is graded. The patchy infiltration pattern in Gaucher's disease consists of localized areas of abnormal marrow (low signal intensity on T1- and T2-weighted SE images) on a background of normal bone marrow (high signal intensity and T1- and T2-weighted SE images). In the diffuse pattern, the bone marrow is completely replaced. The diffuse pattern is considered to reflect a more advanced stage of the disease. Furthermore, the absence of fat in the basivertebral vein region was added as a score, in a binominal fashion (present/absent). The disappearance of fat surrounding the basivertebral plexus was included in the BMB. In the femurs the marrow signal intensities on T1-weighted and T2-weighted images were graded compared to the signal intensity of subcutaneous fat. The intensities were scored as hyperintense, slightly hyperintense, isointense, slightly hypointense, and hypointense. The femurs were divided in three sites of involvement, proximal epiphysis/apophysis, meta-diaphysis, and distal epiphysis.

20.5 Assessment of Outcome and Survival in Patients with Acute Myeloid Leukemia in Complete Remission

Many parameters such as age, karyotype, and performance status are known to be prognostic factors in patients with acute myeloid leukemia (AML) before they receive chemotherapy (Ferrara et al. 2008). If complete remission (CR) is maintained for more than 3 years, the likelihood of relapse is less than 10% (de Lima et al. 1997). To improve the duration of remission, patients at high risk of relapse should be detected as early as possible. DCE-MRI has the potential to noninvasively assess the microvascular structure of bone marrow. Chen et al. examined 51 patients with acute myeloid leukemia in complete remission with DCE-MRI. Semiquantitative parameters (peak and slope) as well as quantitative parameters (amplitude, K_{ep} [efflux rate constant], and K_{el} [elimination constant]) were calculated. It could be shown that high values of peak (≥ 0.41), slope (≥ 0.0235), amplitude (≥ 0.03), and K_{ep} (≥ 0.0082) were associated with shorter overall survival ($p = 0.004$, 0.01, 0.034, and 0.026, respectively). A high value of K_{ep} was also associated with shorter relapse-free survival ($p = 0.008$). After multivariate Cox proportional hazards analysis, only K_{ep} revealed as an independent factor for overall survival (relative risk, 30.305; $p = 0.21$) and relapse-free survival (relative risk, 6.477; $p = 0.009$). K_{ep} (efflux rate constant) measured with tracer kinetic modeling represents the contrast exchange between blood plasma and extravascular extracellular space. It is thought that bone marrow vessels and their endothelium should be normalized with reduced vessel wall permeability in complete remission and therefore show low values of K_{ep}. Increased values for K_{ep} may indicate not adequately normalized vessel permeability and therefore may indicate a high risk of relapse. K_{ep} might serve as a guide for the selection of personalized treatment plans in patients with AML and complete remission (Chen et al. 2011).

20.6 Differentiation of Benign and Malignant Vertebral Fractures

The differentiation of benign and malignant vertebral fractures is a common clinical problem, if there is no adequate trauma anamnesis. Although there exist morphologic MRI criteria in the differentiation of both entities (Frager et al. 1988; An et al. 1995; Cuenod et al. 1996; Shih et al. 1999; Baur et al. 2002; Jung et al. 2003), especially in the first 8–12 weeks after the vertebral fracture, similar appearance of benign and malignant vertebral fractures on T1-w, T2-w, and STIR images due to edema and hemorrhage can mimic malignant findings in a benign osteoporotic vertebral fracture (Moulopoulos et al. 1996). To overcome this diagnostic impairment, quantitative diffusion-weighted imaging and quantitative chemical shift imaging promise to be additional features in determining the nature of an acute vertebral fracture.

Quantitative Diffusion-Weighted Imaging

The apparent diffusion coefficient (ADC) is calculated using two or more images with different diffusion weightings (*b*-values). Acute osteoporotic fractures show an increased diffusion with high values on ADC maps, which is explained by the disruption of the trabecular structure and bone marrow edema in the diseased vertebrae. Pathologic fractures are associated with restricted diffusion, i.e., lower values on ADC maps. In spinal tumors with vertebral body compression fractures, increased tumor cell packing leads to a smaller and more restricted extracellular space, resulting in increased signal from restricted water protons, as has been observed in lytic metastases (Baur et al. 2003). Although the results showed somewhat variable results, the majority of the studies revealed typical ADC ranges associated with normal and pathological bone marrow. Normal bone marrow shows ADCs of 0.2 to 0.5×10^{-3} mm²/s. Metastases or malignant fractures range from ~0.7 to 1.0×10^{-3} mm²/s

(Fig. 20.5), osteoporotic or traumatic fractures show ADCs of ~1.0 to 2.0×10^{-3} mm²/s (Fig. 20.6) (Dietrich et al. 2009).

Biffar et al. examined 24 osteoporotic vertebral fractures and 20 malignant vertebral fractures and showed that DW-ssTSE (*b*-values 100, 250, 400, 600 s/mm²) could significantly discriminate between both entities showing a sensitivity of 65% and specificity of 88% at an ADC of 1.49×10^{-3} mm²/s as a cutoff value. DW-EPI showed no statistical differences due to an underestimated signal attenuation and gross geometrical image distortions caused by susceptibility heterogeneities (Biffar et al. 2010).

Karchevsky et al. performed a meta-analysis and reviewed four studies assessing the ADC values of benign and malignant vertebral fractures. They could show that mean ADC values in benign fractures were significantly higher than malignant fractures with a standardized mean difference (SMD) of 2.8 and a 95% confidence interval for the SMD of 2.1–3.5. Mean ADCs of pathologic fractures and malignant lesions were in the range from 0.19 to 0.853×10^{-3} mm²/s, benign fractures showed ADCs from 0.32 to 1.94×10^{-3} mm²/s (Karchevsky et al. 2008).

Although quantitative diffusion-weighted imaging shows significant differences between benign and malignant vertebral fractures, its specificity is limited due to a remarkable overlap. Although the ADC value itself should be independent from sequence type and sequence parameters, the measured values are influenced by sequence-specific artifacts, range of used *b*-values, application of fat saturation, noise, and perfusion effects. DWI of bone marrow requires considerably more robust imaging techniques than typical MRI of the brain, and therefore it is still a technique on very active research.

Quantitative Chemical Shift (In-/Opposed-Phase) Imaging

Chemical shift imaging uses the different precession frequencies of water and fat protons due to the differences in their molecular environment. The greater the signal intensity loss on
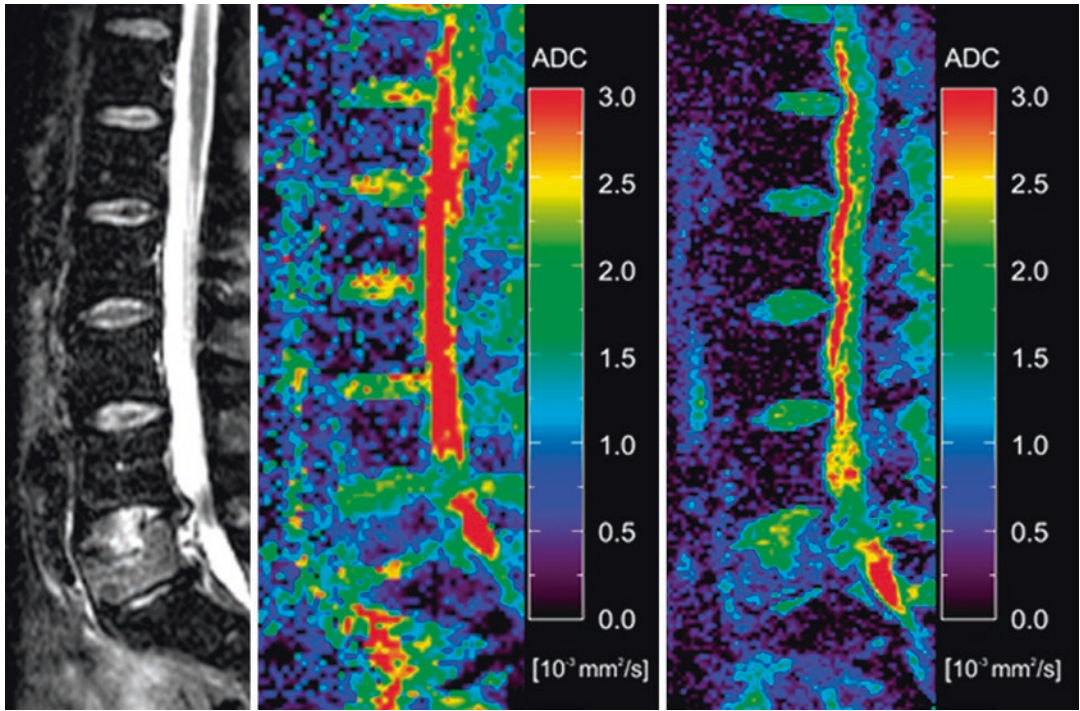
Fig. 20.5 Malignant fracture due to hypopharyngeal cancer: (**a**) STIR image showing edema in the whole vertebral body. Corresponding ADC maps acquired with (**b**) DW-HASTE (mean ADC 0.64) and (**c**) DW-EPI (mean ADC 0.73) showing relatively low values due to high cell packing
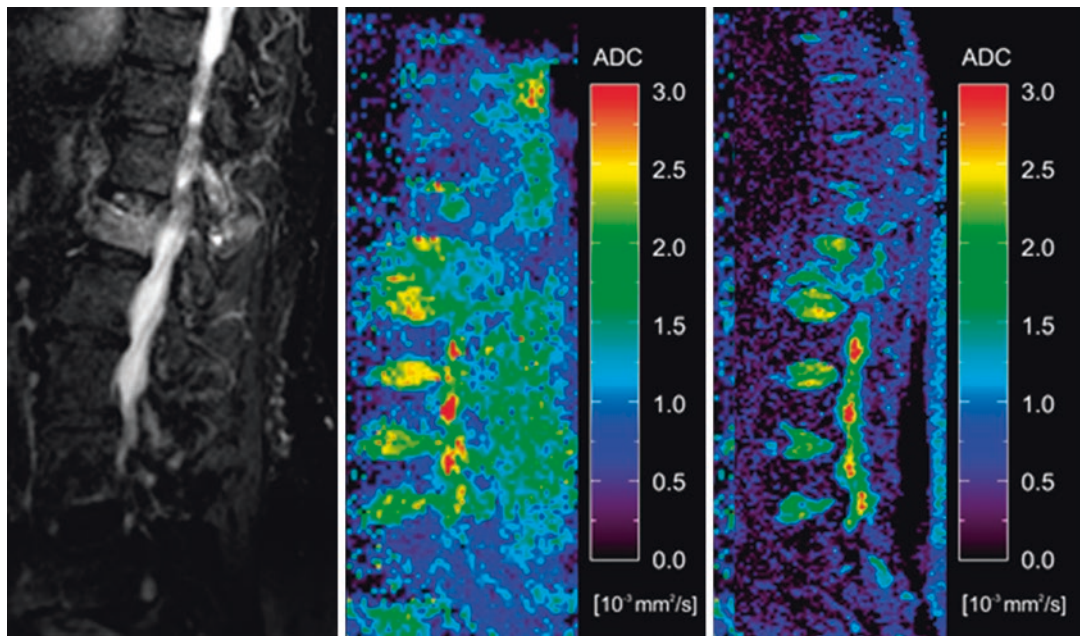

Fig. 20.6 Osteoporotic fracture: (**a**) STIR image showing edema in the whole vertebral body. Corresponding ADC maps acquired with (**b**) DW-HASTE (mean ADC 1.59) and (**c**) DW-EPI (mean ADC 1.41) showing relatively high values due to edema

opposed-phase images compared to in-phase images is, the greater is the fat content in the vertebral bone marrow. If tumor has infiltrated the vertebral bone marrow, the fatty marrow is expected to be displaced, resulting in a lower content of fat, and therefore higher signal inten-sity on opposed-phase images (Fig. 20.7). In osteoporotic vertebral fractures, mostly normal fatty marrow should be detected, without signifi-cant changes in the fat content, resulting in a sig-nal intensity drop, nearly equal to normal bone marrow (Fig. 20.8). The relative signal intensity
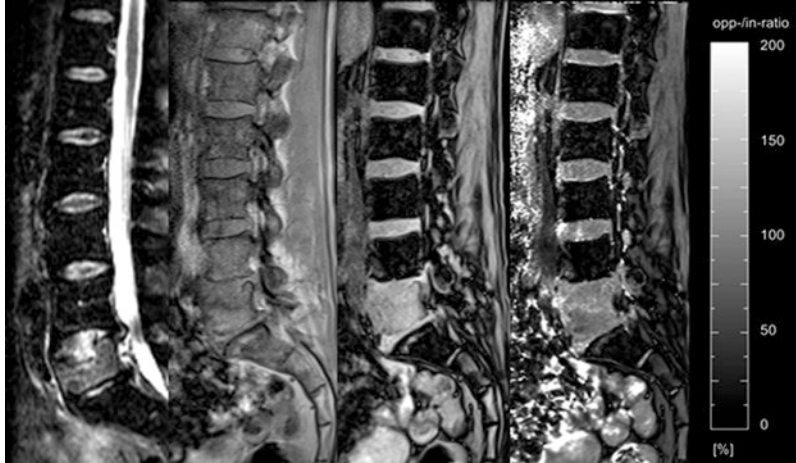

Fig. 20.7 Malignant fracture due to hypopharyngeal can-cer: (**a**) STIR image showing edema in the whole vertebral body. Corresponding (**b**) inphase image showing high sig-nal intensity and (**c**) opposed-phase image also showing high signal intensity in comparison with normal vertebral bone marrow. The opp-/in-ratio is 99%, which means that there is only a slight signal drop of −1% on opposed-phase images compared to inphase images. Note that normal ver-tebral bone marrow has a much lower opp/in-ratio, corre-sponding to a higher signal drop on opposed-phase images

Fig. 20.8 Osteoporotic fracture: (**a**) STIR image show-ing edema in the whole vertebral body. Corresponding (**b**) inphase image showing high signal intensity and (**c**) opposed-phase image showing a low signal intensity, as also shown in normal vertebral bone marrow. The opp-/in-ratio is 69%, which means that there is a high signal drop of −31% on opposed-phase images compared to inphase images, as can also be noted in normal vertebral bone marrow

ratio (signal intensity$_{OP}$/signal intensity$_{IP}$) (Eito et al. 2004; Erly et al. 2006) can be calculated for quantitative measurement.

Studies at 1.5 T revealed mean signal intensity ratios of 0.46 ± 0.14 (SD) for normal vertebral bone marrow (Eito et al. 2004), whereas nonneoplastic fractured vertebrae showed mean intensity ratios of 0.63 ± 0.21 SD (Eito et al. 2004) to 0.58 ± 0.02 SD (Erly et al. 2006), while malignant compression fractures had higher mean signal intensity ratios of 1.02 ± 0.11 SD (Eito et al. 2004) to 0.98 ± 0.095 SD (Erly et al. 2006).

Performing ROC-analysis, a signal intensity ratio of >0.8 indicating malignancy showed best discrimination of benign and malignant vertebral fractures with a sensitivity of 95% and a specificity of 89% (Erly et al. 2006).

Chemical shift imaging is a reliable supportive tool for the differentiation of benign and malignant vertebral fractures. However, if strong edema and reduced fat content are present, the signal intensities can also be high on opposedphase images in osteoporotic fractures. Care should be taken to acquire the same sequence type with the appropriate sequence parameters, since a slight shift, e.g., in TE and flip angle can cause a significant shift in contrast.

References

Aguayo A, Kantarjian H et al (2000) Angiogenesis in acute and chronic leukemias and myelodysplastic syndromes. Blood 96(6):2240–2245

Akkerman EM, Maas M (1995) A region-growing algorithm to simultaneously remove dephasing influences and separate fat and water in two-point Dixon imaging. Proceedings of the Society for Magnetic Resonance in Medicine and the European Society for Magnetic Resonance in Medicine and Biology

An HS, Andreshak TG et al (1995) Can we distinguish between benign versus malignant compression fractures of the spine by magnetic resonance imaging? Spine (Phila Pa 1976) 20(16):1776–1782

Baur A, Bartl R et al (2004) Neovascularization of bone marrow in patients with diffuse multiple myeloma: a correlative study of magnetic resonance imaging and histopathologic findings. Cancer 101(11): 2599–2604

Baur A, Dietrich O et al (2003) Diffusion-weighted imaging of bone marrow: current status. Eur Radiol 13(7):1699–1708

Baur A, Stabler A et al (2002) Acute osteoporotic and neoplastic vertebral compression fractures: fluid sign at MR imaging. Radiology 225(3):730–735

Baur A, Stabler A et al (1997) MRI gadolinium enhancement of bone marrow: age-related changes in normals and in diffuse neoplastic infiltration. Skelet Radiol 26(7):414–418

Biffar A, Baur-Melnyk A et al (2010) Multiparameter MRI assessment of normal-appearing and diseased vertebral bone marrow. Eur Radiol 20(11): 2679–2689

Chen BB, Hsu CY et al (2011) Dynamic contrast-enhanced MR imaging measurement of vertebral bone marrow perfusion may be indicator of outcome of acute myeloid leukemia patients in remission. Radiology 258(3):821–831

Cuenod CA, Laredo JD et al (1996) Acute vertebral collapse due to osteoporosis or malignancy: appearance on unenhanced and gadolinium-enhanced MR images. Radiology 199(2):541–549

de Lima M, Strom SS et al (1997) Implications of potential cure in acute myelogenous leukemia: development of subsequent cancer and return to work. Blood 90(12):4719–4724

Dietrich O, Biffar A et al (2009) Diffusion-weighted imaging of bone marrow. Semin Musculoskelet Radiol 13(2):134–144

Dixon WT (1984) Simple proton spectroscopic imaging. Radiology 153(1):189–194

Eito K, Waka S et al (2004) Vertebral neoplastic compression fractures: assessment by dual-phase chemical shift imaging. J Magn Reson Imaging 20(6):1020–1024

Erly WK, Oh ES et al (2006) The utility of in-phase/opposed-phase imaging in differentiating malignancy from acute benign compression fractures of the spine. AJNR Am J Neuroradiol 27(6):1183–1188

Ferrara F, Palmieri S et al (2008) Clinically useful prognostic factors in acute myeloid leukemia. Crit Rev Oncol Hematol 66(3):181–193

Frager D, Elkin C et al (1988) Subacute osteoporotic compression fracture: misleading magnetic resonance appearance. Skelet Radiol 17(2):123–126

Hollak C, Maas M et al (2001) Dixon quantitative chemical shift imaging is a sensitive tool for the evaluation of bone marrow responses to individualized doses of enzyme supplementation therapy in type 1 Gaucher disease. Blood Cells Mol Dis 27(6):1005–1012

Horger M, Weisel K et al (2011) Whole-body diffusion-weighted MRI with apparent diffusion coefficient mapping for early response monitoring in multiple myeloma: preliminary results. Am J Roentgenol 196(6):W790–W795

Jung HS, Jee WH et al (2003) Discrimination of metastatic from acute osteoporotic compression spinal fractures with MR imaging. Radiographics 23(1):179–187

Karchevsky M, Babb JS et al (2008) Can diffusion-weighted imaging be used to differentiate benign from pathologic fractures? A meta-analysis. Skelet Radiol 37(9):791–795

Maas M, Hollak CE et al (2002) Quantification of skeletal involvement in adults with type I Gaucher's disease: fat fraction measured by Dixon quantitative chemical shift imaging as a valid parameter. AJR Am J Roentgenol 179(4):961–965

Maas M, van Kuijk C et al (2003) Quantification of bone involvement in Gaucher disease: MR imaging bone marrow burden score as an alternative to Dixon quantitative chemical shift MR imaging—initial experience. Radiology 229(2): 554–561

Moulopoulos LA, Maris TG et al (2003) Detection of malignant bone marrow involvement with dynamic contrast-enhanced magnetic resonance imaging. Ann Oncol 14(1):152–158

Moulopoulos LA, Yoshimitsu K et al (1996) MR prediction of benign and malignant vertebral compression fractures. J Magn Reson Imaging 6(4):667–674

Nobauer I, Uffmann M (2005) Differential diagnosis of focal and diffuse neoplastic diseases of bone marrow in MRI. Eur J Radiol 55(1):2–32

Plecha DM (2000) Imaging of bone marrow disease in the spine. Semin Musculoskelet Radiol 4(3):321–327

Pui MH, Mitha A et al (2005) Diffusion-weighted magnetic resonance imaging of spinal infection and malignancy. J Neuroimaging 15(2):164–170

Rahmouni A, Montazel JL et al (2003) Bone marrow with diffuse tumor infiltration in patients with lymphoproliferative diseases: dynamic gadolinium-enhanced MR imaging. Radiology 229(3):710–717

Rajkumar SV, Leong T et al (2000) Prognostic value of bone marrow angiogenesis in multiple myeloma. Clin Cancer Res 6(8):3111–3116

Sezer O, Niemoller K et al (2001) Decrease of bone marrow angiogenesis in myeloma patients achieving a remission after chemotherapy. Eur J Haematol 66(4):238–244

Shih TT, Huang KM et al (1999) Solitary vertebral collapse: distinction between benign and malignant causes using MR patterns. J Magn Reson Imaging 9(5):635–642

Stabler A, Doma AB et al (2000) Reactive bone marrow changes in infectious spondylitis: quantitative assessment with MR imaging. Radiology 217(3):863–868

Vacca A, Ribatti D et al (1994) Bone marrow angiogenesis and progression in multiple myeloma. Br J Haematol 87(3):503–508

Vande Berg BC, Lecouvet FE (2005) Normal variants and frequent marrow alterations that simulate bone marrow lesions at MR imaging. Radiol Clin N Am 43(4):761–770. ix